A photometric and spectroscopic study of dwarf and giant galaxies in the Coma cluster - II. Spectroscopic observations [1]

Bahram Mobasher,[2,3] Terry J. Bridges,[4] Dave Carter,[5] Bianca M. Poggianti,[6] Y. Komiyama,[7] N. Kashikawa,[8] M. Doi,[9] M. Iye,[8] S. Okamura,[10,11] M. Sekiguchi,[12] K. Shimasaku,[11] M. Yagi,[8] N. Yasuda[8]

2) Space Telescope Science Institute, 3700 San Martin Drive, Baltimore, MD 21218, USA

3) Affiliated with the Space Sciences Department of the European Space Agency

4) Anglo-Australian Observatory, PO Box 296, Epping, NSW 2121, Australia

5) Astrophysics Research Institute, Liverpool John Moores University, Twelve Quays House, Egerton Wharf, Birkenhead, Wirral, CH41 1LD, UK

6) Osservatorio Astronomico di Padova, vicolo dell'Osservatorio 5, 35122 Padova, Italy

7) Subaru Telescope, 650 North Aohoku Place, Hilo, HI 96720, USA

8) National Astronomical Observatory, Mitaka, Tokyo, 181-8588, Japan

9) Institute of Astronomy, School of Science, University of Tokyo, Mitaka, 181-0015, Japan

10) Research Center for the Early Universe, School of Science, University of Tokyo, Tokyo 113-0033, Japan

11) Department of Astronomy, University of Tokyo, Bunkyo-ku, Tokyo 113-0033, Japan

12) Institute for Cosmic Ray Research, University of Tokyo, Kashiwa, Chiba 277-8582, Japan

ABSTRACT

This is the second paper in a series studying the photometric and spectroscopic properties of galaxies of different luminosities in the Coma cluster. We present the sample selection, spectroscopic observations and completeness functions. To study the spectral properties of galaxies as a function of their local environment, two fields were selected for spectroscopic observations to cover both the core (Coma1) and outskirts (ie. south-west of the core and centered on NGC4839)- (Coma3) of the cluster. To maximise the efficiency of spectroscopic observations, two sub-samples were defined, consisting of 'bright' and 'faint' galaxies, both drawn from magnitude-limited parent samples. Medium resolution spectroscopy (6-9 Å) was then carried out for a total of 490 galaxies in both fields (302 in Coma1 and 188 in Coma3), using the WYFFOS multi-fiber spectrograph on the William Herschel Telescope. The galaxies cover a range of $12 < R < 20$, corresponding to $-23 < M_R < -15$ ($H_0 = 65$ km/sec/Mpc. The redshifts for these galaxies are measured with an accuracy of 100 km/sec.

The spectral line strengths and equivalent widths are also measured for the same galaxies and analysed in Poggianti et al (2001- paper III). A total of 189 (Coma1) and 90 (Coma3) galaxies are identified as members of the Coma cluster. An analysis of the colors show that only two members of the Coma cluster in our sample have $B - R > 2$. The completeness functions for our sample are calculated. These show that the 'bright sample' is 65% complete at $R < 17$ mag, becoming increasingly incomplete towards fainter magnitudes, while the 'faint sample' follows a monotonically decreasing completeness function at $R > 19$ mag.

Subject headings: galaxies: clusters—galaxies: clusters: individual(Coma)—galaxies:distances and redshifts— galaxies:kinematics and dynamics

1. Introduction

In this series of papers we present the results from a wide-area photometric and spectroscopic survey of galaxies at the core and outskirts of the Coma cluster. In the first paper details of the photometric observations and data reduction are discussed (Komiyama et al 2001; paper I). This is the second paper in the series, presenting the spectroscopic sample selection, observations and completeness functions. The third paper performs an analysis of the diagnostic line indices for the entire spectroscopic sample (Poggianti et al 2001a). Using the spectroscopic data here, a study of the ages of elliptical and S0 galaxies is also carried out (Poggianti et al 2001b). The future papers in this series present spectroscopic comparison with galaxies in intermediate redshift clusters, study of the color-magnitude relation at the core and outskirts of the Coma cluster and the source of its scatter, luminosity function of galaxies in the Coma and its dependence on the local environment and a study of the spatial distribution and dynamics of galaxies in this cluster.

Clusters of galaxies provide ideal environments for studying formation and evolution of galaxies. By studying galaxies located at the center and outer regions of a single cluster, one expects to minimise the parameter space, affecting their evolutionary properties, only to those of the local density. This also provides a continous sequence for study of galaxy evolution from dense (cores of clusters) to less dense (outskirts of clusters) and general field. However, due to technological limitations, caused by small format CCDs, such studies

[1]Based on observations made with the William Herschel Telescope operated on the island of La Palma by the Isaac Newton Group in the Spanish Observatorio del Roque de los Muchachos of the Instituto de Astrofisica de Canarias.

have so far been concentrated only to distant clusters ($z > 0.4$), where only the bright-end of the luminosity function could be sampled (Dressler et al. 1999; van Dokkum et al 1998). For these clusters, one also has the addtional problem of obtaining medium and high resolution spectroscopic data for a statistically significant number of galaxies over a wide range in luminosity. Moreover, it is not clear if the evolutionary history of galaxies in the intermediate to high redshift clusters are indeed similar to those observed in the local Universe, indicating the need for a detailed study of the physical properties of galaxies at the core and outskirts of nearby clusters. In recent years, such investigation has become possible due to the advent of mosaic CCDs and multi-object fiber spectrographs, allowing photometric and spectroscopic observations over large solid angles.

Given the above requirements, we started a large photometric and spectroscopic survey of galaxies at both the core and outskirts of the Coma cluster. The aim of this is to perform a detailed study of the photometric (luminosity, surface brightness, color) and spectroscopic (indices sensitive to metallicity and star-formation) parameters for galaxies at different radial distances from the center of a rich local cluster (ie. the Coma). There are two main differences between the present and previous such studies. Firstly, this covers a significantly larger area than previous spectroscopic surveys of the Coma cluster, providing homogeneous dataset for a large sample at different environments. Secondly, it extends the medium resolution spectroscopy of galaxies to faint luminosities ($R \sim 19-20$), allowing comparison of properties of galaxies in the range $12 < R < 20$ (corresponding to $-23 < M_R < -15$ for $H_0 = 65$ Km/sec/Mpc).

A summary of the photometric observations followed by spectroscopic sample selection and spectroscopic observations are presented in section 2. Section 3 presents the selection function for the spectroscopic sample in this study. This is followed in section 4 by a summary of the main results.

2. Observations

2.1. Photometry

The photometric observations and data reduction are explained in detail in paper I. Briefly, a total area of 2.22 deg.^{2} was surveyed, with a sub-area of 1.375 deg^2 covered in both the B and R bands. This consists of five contiguous fields at the core and outskirts of the Coma cluster. The observations were carried out in the Johnson B and Cousins R bands and are complete to $R = 21$ mag ($B = 22.5$ mag.). To allow for a statistical estimate of the background contamination, a control field (SA57) close to the Coma cluster was also

observed under similar conditions and to the same depth.

Source detection was carried out using the 'connected pixel' algorithm. An object is entered into the catalogue if it extends over a number of connected pixels larger than a threshold value (taken to be 30), with all the pixels having values above the detection threshold (1.5 σ_{sky}). Detailed discussion of source detection and star/galaxy separation is given in paper I. Photometric catalogues were then constructed for each field, consisting of the magnitude (isophotal, aperture, Petrosian), surface brightness (mean, effective), radius (effective, Petrosian, Kron) and the compactness parameter. In this paper, we use the magnitudes measured over a circular aperture of diameter 3 times the Kron radius, r_k. This is an intensity-weighted radius defined as

$$r_k = \frac{\sum_i (r_i \times I_i)}{\sum_i I_i}$$

where r_i and I_i are respectively, the radius and intensity of the ith pixel, with the summations over all pixels above the detection threshold. This has the advantage of scaling magnitudes proportional to the size of the galaxies (using larger apertures for larger galaxies) and hence, measuring the light from all of the galaxy (bulge+disk). $B-R$ colors are also determined over an aperture of diameter $3 \times r_k$ and agree within 2% with those measured over a fixed aperture of 10 arcsec. diameter. Both magnitudes and colors are close to the total values. The estimated photometric accuracy of the present data is 0.03 mag (R-band), 0.04 mag (B-band) and 0.05 mag ($B-R$) as estimated from repeated observations of galaxies which lie in the overlapping regions between the contiguous fields. The astrometry, performed with the APM, is accurate to better than 0.5 arcsec, sufficient for the fiber spectroscopy discussed in the next section.

Two fields (each 32.5×50.8 arcmin) were selected for medium resolution fiber spectroscopy. These were chosen to cover areas with large density contrasts, consisting of the core field at the cluster center (Coma1) and a field south-west of the cluster, centered on NGC4839 and the X-ray secondary peak (Coma3). The coordinates of the centers of the two spectroscopic fields and the total number of galaxies detected in each field to the magnitude limit of the sample are listed in Table 1. The criteria used for selecting the sample for spectroscopic observations are discussed in the next section.

2.2. Selection criteria for the spectroscopic sample

The aims of the spectroscopic observations are to identify members of the cluster in the Coma1 and Coma3 fields and to measure their spectral line indices. The latter requires

medium resolution spectroscopy of galaxies which are confirmed members of the Coma cluster. In order to maximise the efficiency of spectroscopic observations, different criteria were used for selecting galaxies by dividing the photometric sample into two broad classes. First: galaxies which already have redshifts from other studies and are spectroscopically confirmed members of the Coma cluster. These are mostly high luminosity galaxies to which we refer as the 'bright sample'. Second: objects with no available redshifts which are, on average, fainter than the first group. This is referred to as the 'faint sample'. Therefore, the aim of the medium resolution fiber spectroscopy is to measure the spectroscopic line indices for galaxies in the bright sample (which all are confirmed cluster members) and determine both redshifts and line indices for galaxies in the faint sample. Different selection criteria used for the two samples are explained in detail below.

a). The bright spectroscopic sample: This sample was taken from the compilation in Colless & Dunn (1996), and an unpublished list of redshifts for Coma galaxies kindly provided by M. Colless. As this compilation is rather inhomogeneous, using objects with different selection criteria, it is important to investigate possible sources of bias which could be reflected in our spectroscopic sample.

The catalogue by Colless & Dunn (1996), consisting of 552 redshifts, is selected from the photographic plate survey by Godwin, Metcalfe and Peach (1983), which is a magnitude limited sample. This includes redshifts measured by these authors and those compiled from Kent & Gunn (1982), van Haarlem et al (1993) and Caldwell et al (1993). We checked these samples and apart from Caldwell et al, which mainly contains early-type galaxies, did not find evidence for any morphological bias. As the Caldwell et al. sample only constitutes a small fraction of the present survey (2%), this is not expected to introduce a bias in the final spectroscopic catalogue. However, it is possible that the spectroscopic sample is slightly biased against late-type galaxies which, on average, have a fainter characteristic luminosity than the early-type systems. Apart from this, there is no known bias in terms of morphological type or color in this sample. Therefore, we consider this a magnitude limited sample with no significant bias.

From the compiled sample, a total of 257 and 123 galaxies were found to be in the Coma1

Table 1: Coordinates of the centers of the two spectroscopic fields in Coma

	RA(J2000)	Dec(J2000)	n
Coma1 (center field)	12h 59m 45.17s	27° 57′ 53.1″	2744
Coma3 (NGC4839 field)	12h 57m 28.48s	27° 08′ 08.5″	2210

and Coma3 fields respectively. All the galaxies in this sample have $R < 18$ mag, with their R-band magnitude and $B - R$ color distributions presented in Figure 1. The candidates for spectroscopic observations were then selected to have a uniform distribution over the magnitude range covered by their parent sample. These consist of 138 and 85 galaxies in Coma1 and Coma3, respectively. The magnitude and color distributions for these galaxies, also presented in Figure 1, show a similar distribution as their parent sample.

In order to make the maximum use of the fiber configurations, a few spare fibers were assigned to objects with $R < 18$ mag. and no available redshifts. These objects, which are selected randomly, were included where no source with spectroscopically confirmed membership was available.

b). The faint spectroscopic sample: The 'faint sample' for spectroscopic observations was selected from the photometric survey described in paper I, based on their colors and magnitudes. The $(B-R)-R$ color-magnitude diagram for galaxies in the entire photometric survey of Coma1 and Coma3 fields is presented in Figure 2. The objects in the faint sample are selected to satisfy $17.5 < R < 20$ (corresponding to $-17.5 < M_R < -15$) and $1 < B-R < 2$. The area covered by these galaxies in the color-magnitude diagram is shown in Figure 2 by a rectangle. The brighter magnitude limit is adopted to allow dwarf galaxies into the sample while the color boundaries eliminate a large fraction of non-cluster galaxies (Secker 1996). The slight overlap in magnitude between the 'bright' and 'faint' samples allows inclusion into the spectroscopic sample of some relatively bright galaxies ($R \sim 17.5$) for which redshifts are not available. The faint magnitude limit is set by the completeness requirement and feasibility in getting the required S/N in a reasonable exposure time. To explore the nature of galaxies satisfying this requirement and the effect of our color selection criteria, we compute the spectral energy distributions and colors for models with a broad range of star-formation histories, mimicking ellipticals, spirals (of types Sa, Sb, Sc and Sd), and galaxies with a current starburst at $z = 0.023$ (the redshift of the Coma cluster)- (Barbaro & Poggianti 1997). The metallicity evolution was taken into account, so that the models of the later types have a lower average metallicity than those of the earlier types. All but the starburst models are found to have colors redder than our blue cut-off ($B - R > 1$). Therefore, the color boundaries adopted for the faint sample here would *only* exclude the starbursts (if present). Figure 2 shows that there are 22 galaxies with $B - R < 1$ and $17.5 < R < 20$, constituting only 5% of the total spectroscopic sample (this is the fraction which one would miss by imposing the $B - R$ color criteria adopted here).

A total of 222 and 190 galaxies in Coma1 and Coma3 satisfy these criteria. The R-band magnitude and B-R color distributions for galaxies in this sample are shown in Figure 3. The spectroscopic candidates were selected randomly from this parent sample, consisting

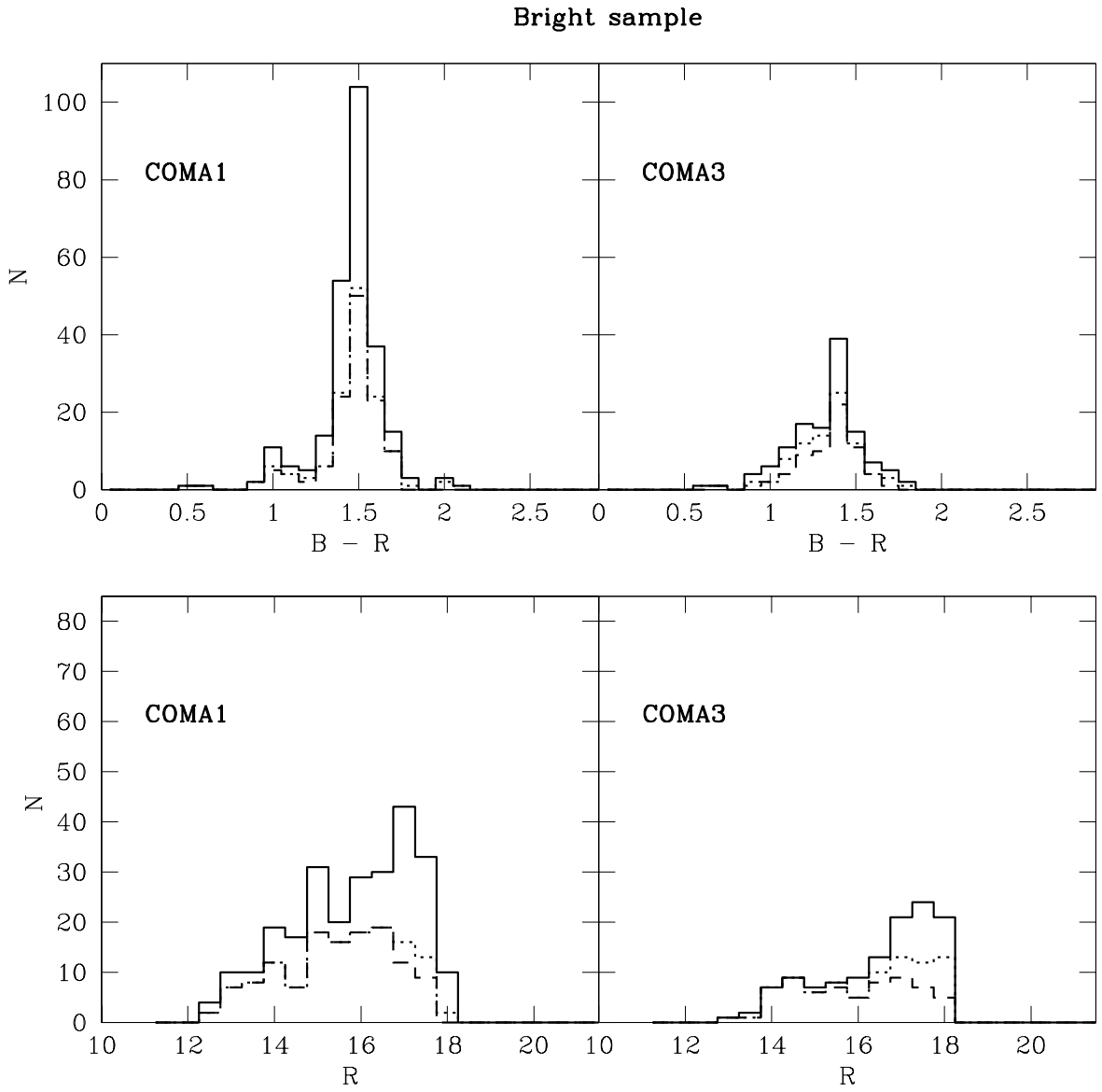

Fig. 1.— R-band magnitude and $B - R$ color distributions for galaxies in the bright spectroscopic sample in the Coma1 and Coma3 fields. The histograms correspond to the parent sample from which the spectroscopic candidates were selected (all confirmed members of the Coma cluster)- (solid line); the objects drawn from the parent sample for medium resolution spectroscopic observations (dotted line); objects for which redshifts and spectral line strengths were obtained (dashed line).

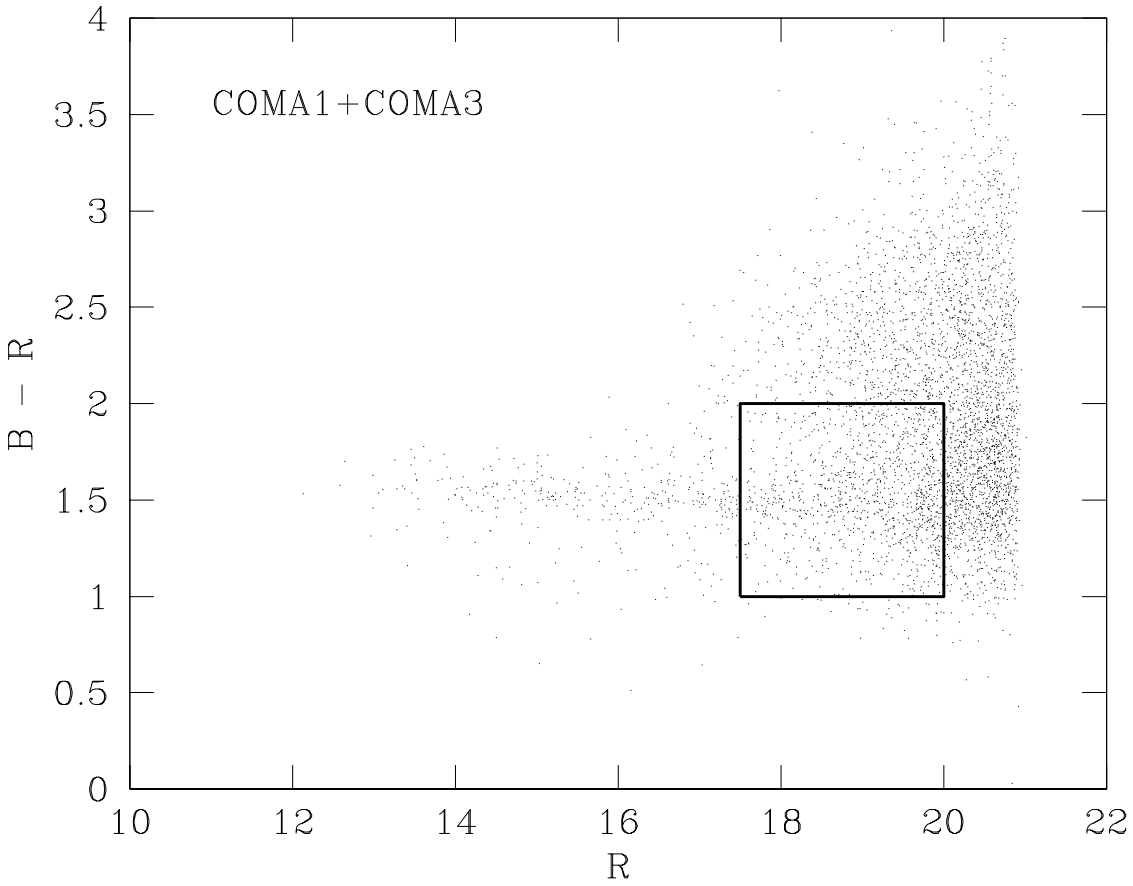

Fig. 2.— R vs. B-R color-magnitude diagram for the *full* photometric survey in the Coma1 and Coma3 fields. The rectangle represents the expected domain for members of the Coma cluster in the faint sample (see text for details).

of a total of 83 and 79 galaxies in Coma1 and Coma3 fields respectively. The restricting factor in selecting the spectroscopic candidates from the parent sample here was the total number of fibers which could be allocated to the objects in a given configuration and the longer exposure time required for galaxies in the faint sample. The magnitude and color distributions for these galaxies are also presented in Figure 3, where they show a similar distribution to that of their parent sample.

To further test the selection criteria for the faint sample here, the color condition was relaxed to explore if any Coma cluster member could be excluded from the spectroscopic sample due to its color. This has the effect of allowing objects with $B-R<1$ and $B-R>2$ into the sample and exploring if such galaxies could indeed be members of the Coma cluster. This is done by first removing the $B-R$ color constraint in the selection of galaxies in the faint sample, and then randomly choosing the candidates for spectroscopic observations. The magnitude and color distributions for galaxies in this sub-sample are presented in Figure 4 for Coma1 (81 galaxies) and Coma3 (24 galaxies) fields. This constitutes all the galaxies for which reliable spectroscopic data (redshifts and spectral line strengths) were measured. The distribution of galaxies in this sample which are spectroscopically confirmed members of the Coma cluster (see section 2.3) are also presented in Figure 4 and show that there are *only* two members of the Coma cluster (67822 and 102739) with $B-R>2$ in our sample. These are galaxies 67822 and 102739, with $B-R=2.139$ and 2.422 respectively. However, the $B-R$ colors for these objects over 10 arcsec diameter apertures are 1.638 (for 67822) and 1.704 (for 102739). These are both substantially bluer than the $B-R$ colors used here, which are measured over an aperture of diameter 3 times the Kron radius, indicating strong color gradients in these objects. This confirms that the adopted color criteria here do not bias against galaxies which are members of the Coma cluster.

The total number of galaxies in the spectroscopic sample in Coma1 and Coma3, and those identified as cluster members (Section 2.4) are listed in Table 2. The spatial distribution of galaxies in all three spectroscopic sub-samples discussed above are presented for both the Coma1 and Coma3 fields in Figure 5.

The reason for dividing the spectroscopic sample in this study into two bright and faint samples was two-fold. Firstly, this increases the efficiency of the spectroscopic observations by allowing different exposure times for the two sub-samples in fiber-spectroscopic observations. Secondly, this allows separation of the spectroscopic sample into giant (bright) and dwarf (faint) sub-samples. A study of the spectroscopic properties of dwarf galaxies compared to giants will then be possible. However, the criteria used to define the bright and faint samples here are independent from galaxy surface brightness. Also, the technique used to identify the dwarf and giant galaxies in paper III is only based on their magnitudes, with no

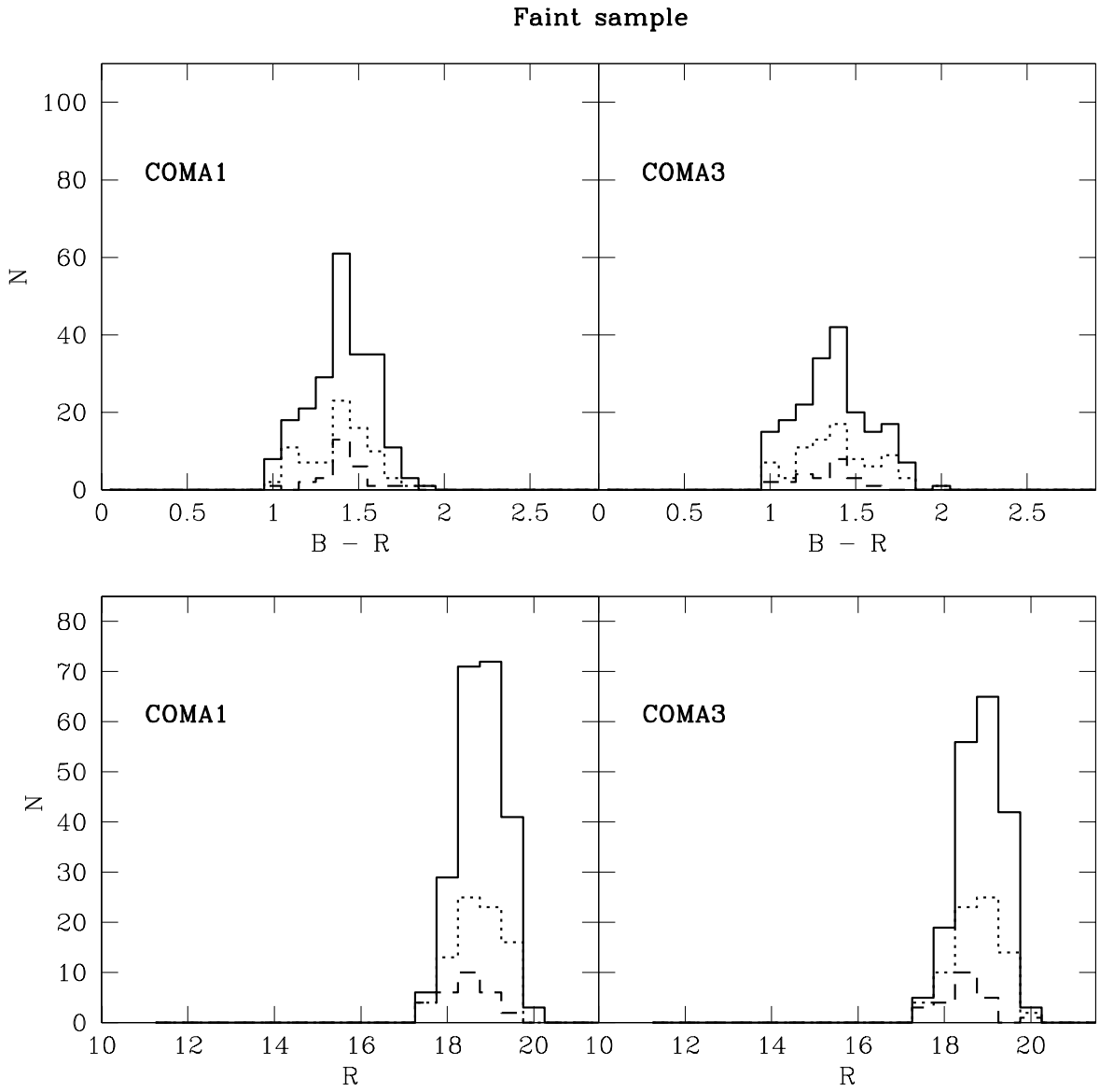

Fig. 3.— R-band magnitude and $B - R$ color distributions for the faint sample in Coma1 and Coma3 fields. The histograms correspond to the parent sample (selected as discussed in the text)-(solid line); objects randomly selected from the parent sample and for which spectroscopic observations were obtained (dotted line); spectroscopically confirmed members of the Coma cluster (dashed line).

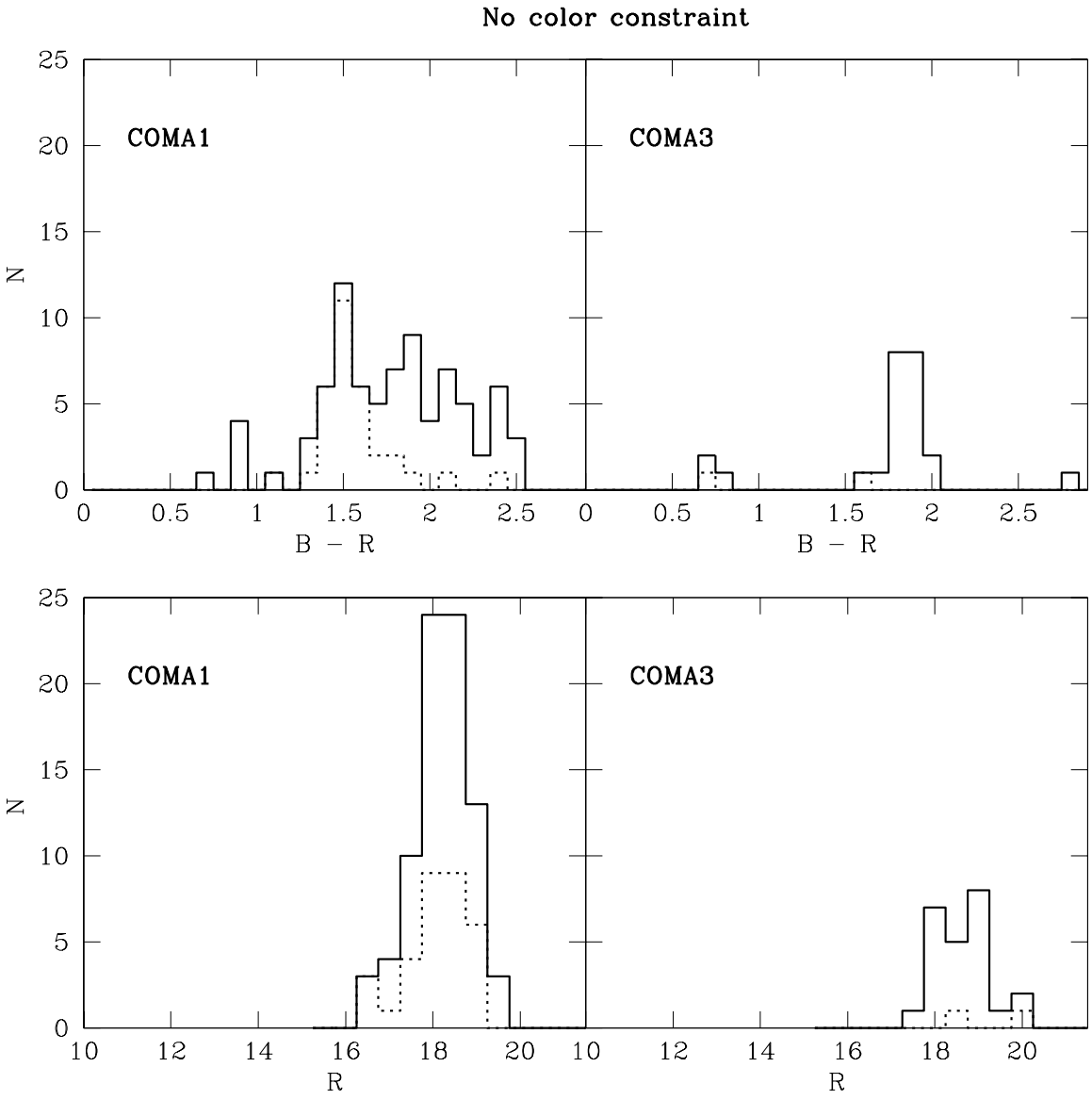

Fig. 4.— R-band magnitude and $B - R$ color distributions for galaxies from the sample for which the color constraint was removed. Objects in both the Coma1 and Coma3 fields are shown. The solid line corresponds to the distribution for the entire sample for which spectroscopic data were obtained. The dotted line corresponds to objects which are spectroscopically confirmed members of the Coma cluster.

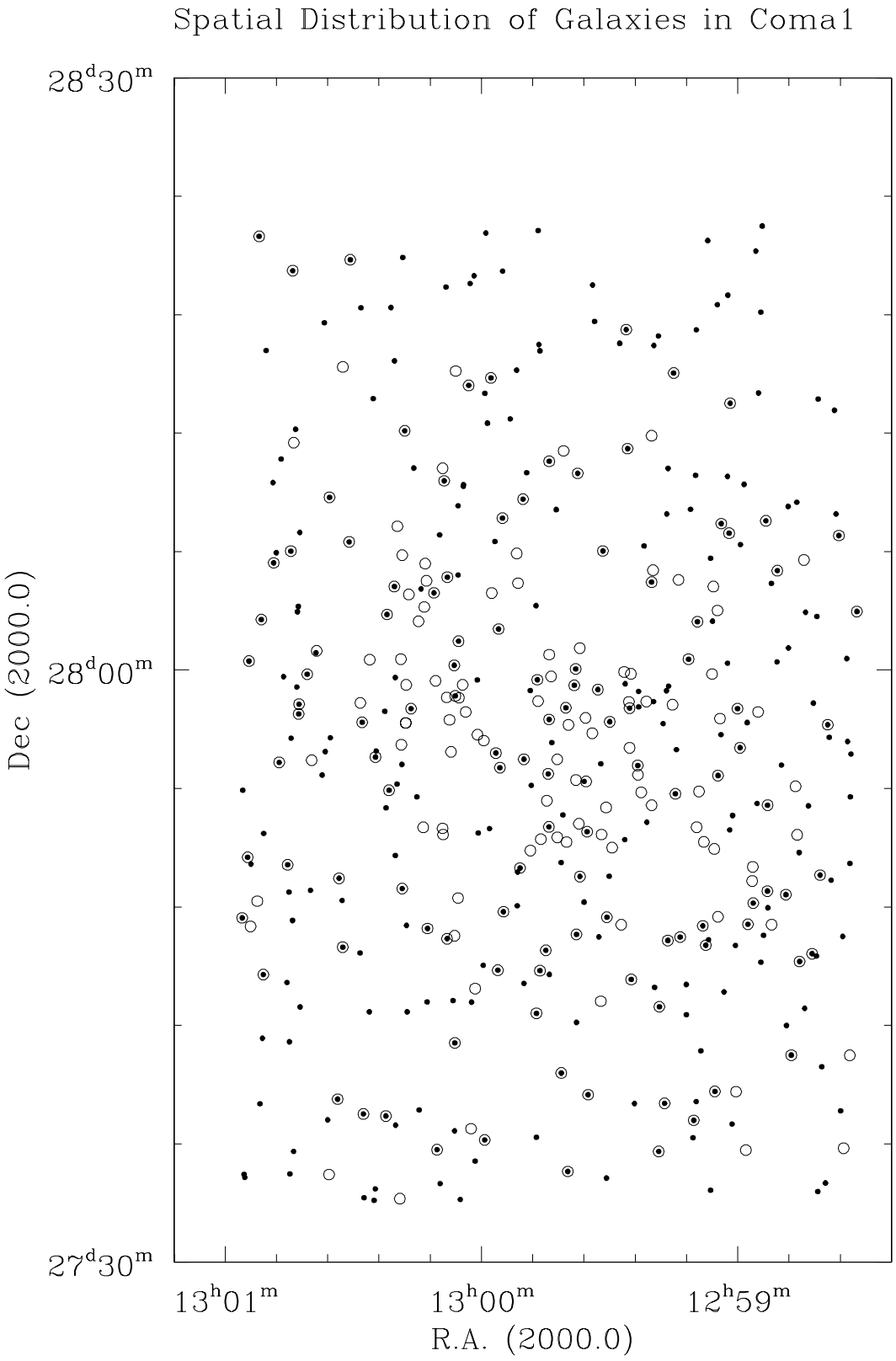
Spatial Distribution of Galaxies in Coma1
28d30m
28d00m
27d30m
Dec (2000.0)
13h01m
13h00m
12h59m
R.A. (2000.0)

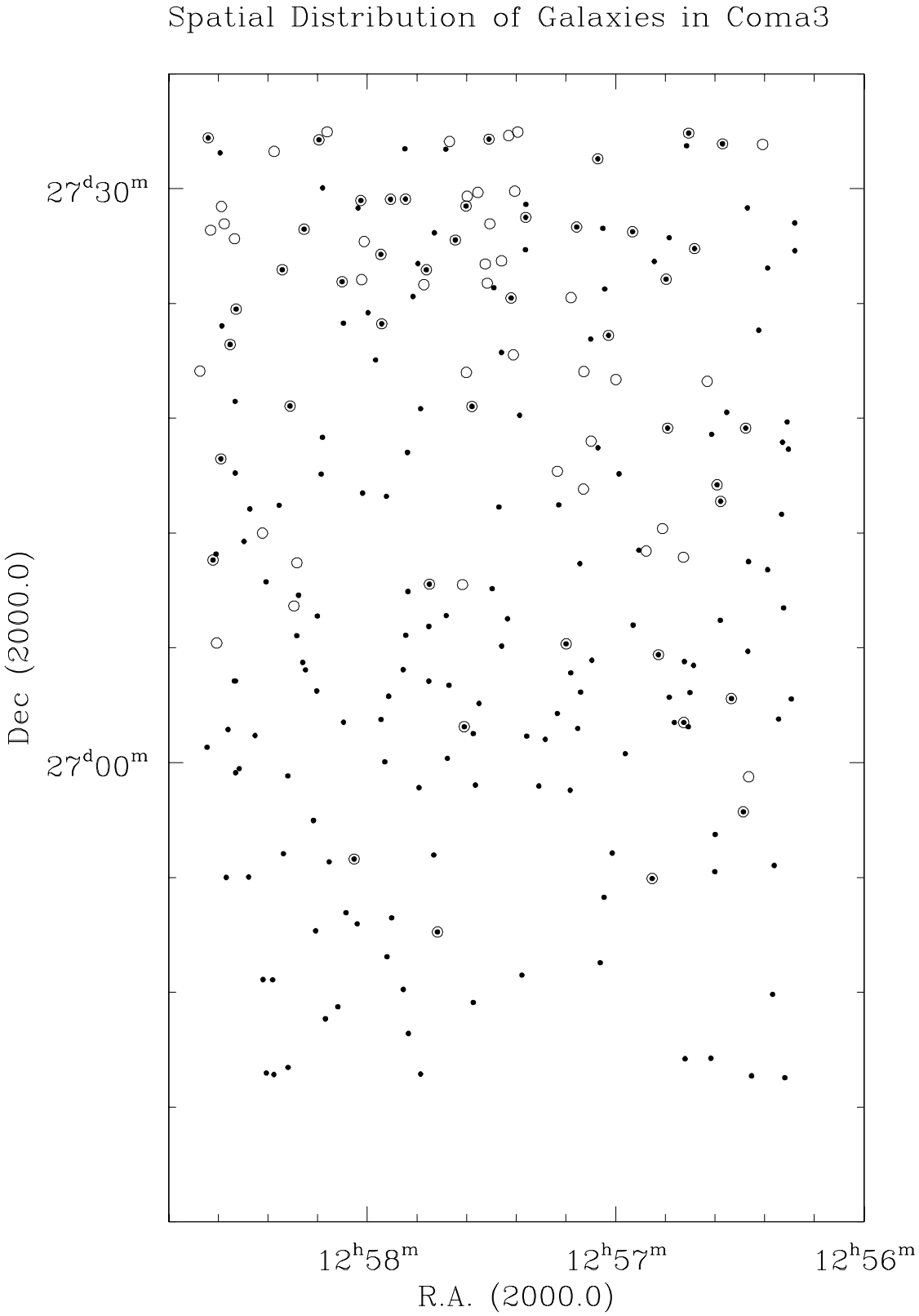

Fig. 5.— Spatial distribution of galaxies for which medium resolution spectroscopy was obtained. This includes objects with spectroscopic data from the present study (filled circles), objects with available spectroscopic redshifts from Colless & Dunn (open circles), and objects

surface brightness-based classification. As dwarfs have, on average, a lower surface brightness than the giants, one expects this to provide an independent test of the above classification schemes. The effective surface brightness for galaxies in this sample are measured in paper I by assuming the Kron magnitude to correspond to the total magnitude of galaxies and hence, estimating the effective radius (the radius containing half the total light of galaxy) for each galaxy. The mean surface brightness inside the effective radius of a galaxy is then measured and used as the effective surface brightness. The R-band effective surface brightness distributions for galaxies in the bright and faint spectroscopic samples are compared in Figure 6. This confirms that the bright sample has a fairly wide range in effective surface brightness ($19 < \mu_R^e < 23.5$), implying that there is no strong surface brightness related bias in this sample. However, for the faint sample, the relatively narrower range covered in surface brightness is likely caused by a bias due to the magnitude limit of this sample, which excludes galaxies with $\mu_R^e > 24$ mag./arcsec^2.

2.3. Spectroscopic Observations and Data Reduction

The spectroscopic observations for this sample were obtained with the WYFFOS multi-fibre spectrograph on the William Herschel Telescope (WHT) on La Palma during April 18-23, 1998. WYFFOS has ~ 110 fibres of 2.7 arcsec diameter coupled to a bench-mounted spectrograph of Baranne design (e.g. Bridges 1998). We allocated typically 60-70 objects to fibers in a given configuration, and on average, 15-20 sky fibers. The 600B grating was used, giving a dispersion of ~ 3 Å/pixel, a total spectral coverage of ~ 3000 Å with a TEK 1024^2 CCD, and a resolution varying between 6–9 Å FWHM, depending on location on the CCD. Our spectra were centered on 5100 Å, thus covering many interesting spectral features ranging from Ca H&K in the blue to NaD in the red.

The galaxies were divided into different configurations, depending on their luminosities. A total of 10 configurations were executed for the Coma1 and Coma3 fields, with total exposure times of 3 hours for the faint sample and 1 hour for the bright sample. Argon lamps for wavelength calibration and offset sky exposures for fibre throughput calibration were also obtained. We also observed spectroscopic flux standards, Lick standards, and radial velocity standards during twilight. The reduction of these multi-fibre spectra was performed using the dedicated `wyfred` package.

Twilight sky flats or combined object frames were used to define the apertures and trace the spectra on the CCD. The median offset sky exposures were then used to calculate the throughput for each fibre, and to normalize all of the sky fibres. The arc spectra were extracted and matched with arc lines to determine the dispersion solution. The fibre median

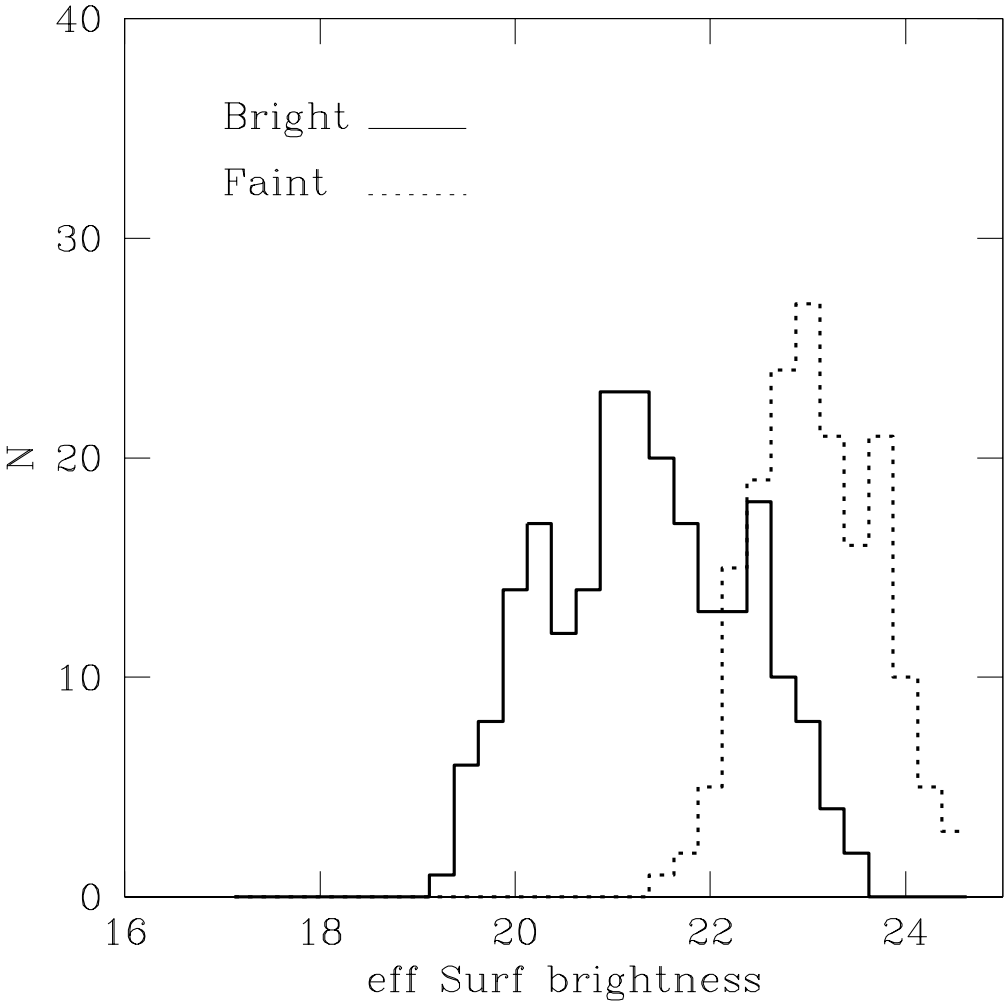

Fig. 6.— Distribution of the R-band effective surface brightness for the bright sample (solid line), dominated by giant galaxies, compared to the distribution for the faint sample (dotted line), dominated by the dwarfs.

rms ranged between 0.15–0.2 Å ($\sim$ 1/20 of a pixel). Finally, the object spectra were extracted, normalized, and wavelength calibrated. The sky subtraction was performed using a master sky spectrum, constructed by combining the normalized sky spectra. The sky subtraction accuracy was quite good, ranging between 1–3% (defined as the *rms* of the normalized sky fibres about the master sky spectrum). Sample spectra of galaxies with different luminosities in the bright and faint samples are shown in Fig. 7.

The spectra were flux calibrated using standard FIGARO procedures on the spectra of the flux standards, obtained on 5 of the 6 nights. Each flux standard was observed through one fibre only. As a result, fibre to fibre variations in throughput as a function of wavelength will cause some small systematic errors in the final flux calibrated spectrum. Comparison between the flux calibration curves derived from the flux standards obtained on the 5 nights shows errors of up to 20% in the *relative* flux at the two ends of the spectrum (4000 and 6500 Å). This could be due to a relative difference in fiber throughput as a function of wavelength. Our spectral indices are of course determined over much shorter regions of the spectrum, with continuum passbands on either side of the feature, and hence are not seriously affected by this.

2.4. Velocity Measurements

Velocities are needed in this study to determine membership in the Coma cluster (for the faint sample), and to measure the *rest-frame* spectral indices (for all the objects). For galaxies with emission lines, velocities were determined from the average of all measureable emission lines. For those objects without emission lines, velocities were obtained by cross-correlating against the radial velocity template stars hd65934, hd86801, and hd90861. We used the IRAF `fxcor` Fourier cross-correlation package, masking out regions of the spectra affected by night-sky lines. The final velocity was taken as that of the template with the highest cross-correlation (Tonry & Davis 1977) coefficient. Those with cross-correlation coefficients < 2 were not used. For objects with both emission and absorption lines, we checked to ensure that there were no significant shifts between emission and absorption line velocities.

As an external check on the accuracy of our velocities, the redshifts for Coma cluster galaxies in the present survey are compared with redshifts for the same galaxies by Colless & Dunn (1996). There are a total of 147 (Coma1) and 44 (Coma3) galaxies in common between the two surveys. The difference between the velocities estimated in the two studies is plotted in Figure 8 as a function of R-band magnitude and $B-R$ color. This shows a mean difference of $< V_{this\ study} - V_{CD} >= 22$ km/sec (Coma1) and 30 km/sec (Coma3) with

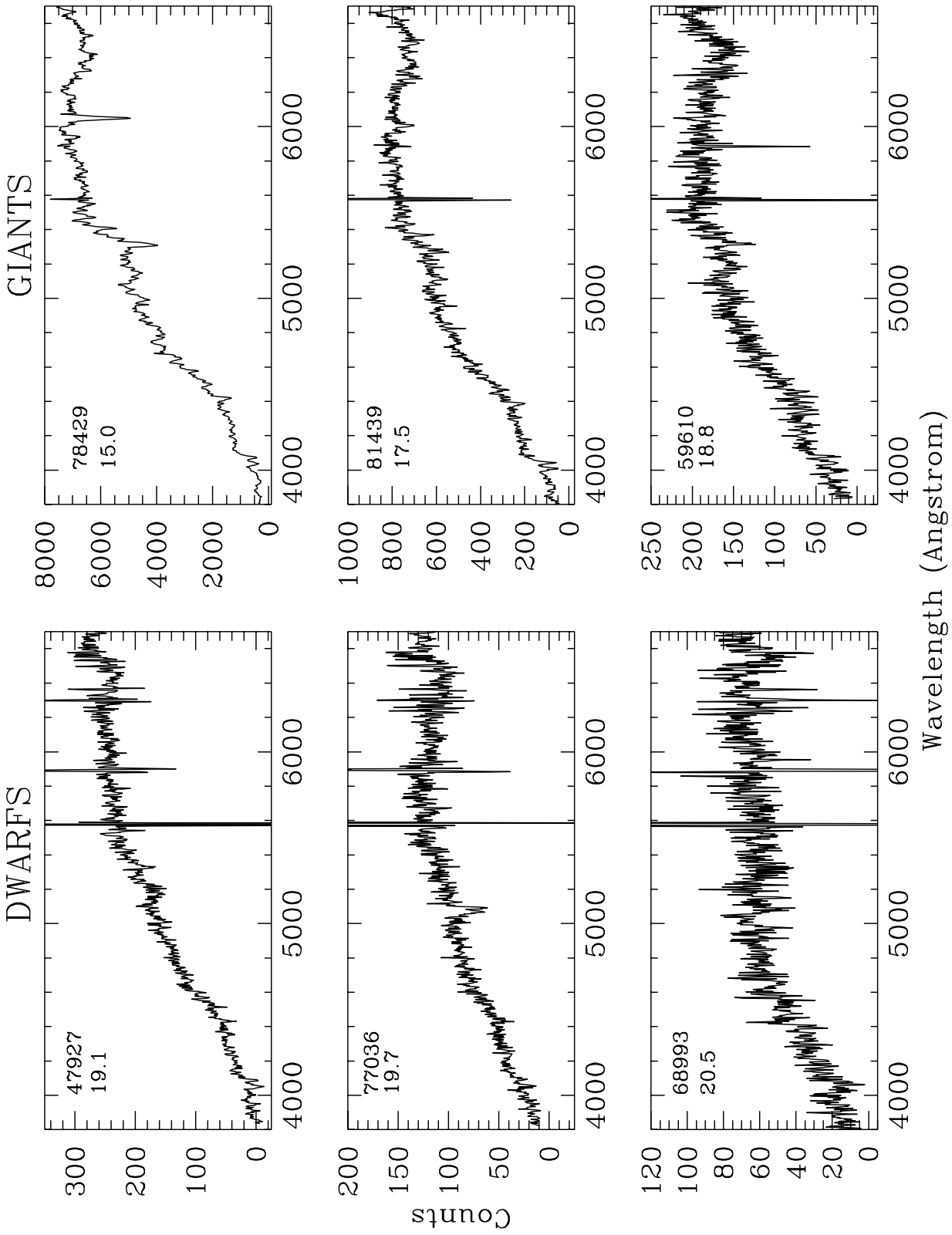

Fig. 7.— Sample spectra of galaxies in the faint (left hand side) and bright (right hand side) samples. The order is from high S/N to low S/N from top to bottom. The object IDs are shown on each panel.

no dependence on galaxy magnitude or color.

Assuming a Gaussian distribution of velocity differences, an *rms* of 101 km/sec is found. Therefore, an error of 100 km/sec is taken for the velocities of the Coma galaxies in this study, consistent with that expected for our spectral resolution and S/N. This error corresponds to the velocities estimated for galaxies in the bright sample, as the comparison in Figure 8 is mostly dominated by these objects. The faint sample has a relatively lower S/N, and the velocity uncertainties will likely be higher. Measurement of the spectral line indices and their associated errors will be discussed in detail in paper III.

The redshift distributions for *all* the galaxies with spectroscopic data from this study are presented in Figure 9. This consists of the bright and faint samples (Figures 9a and 9b) and the sub-sample selected with no $B-R$ color criteria (Figure 9c). Taking a mean velocity of 7000 km/sec and a dispersion of 1000 km/sec for galaxies in the Coma cluster (Colless & Dunn 1996), we define a 3σ cut corresponding to a velocity range of $4000 < \mathrm{V} < 10{,}000$ km/sec for galaxies in order to be included as members of the Coma cluster. This is clear in the peak in the redshift distribution in Figure 9. All the galaxies which are identified as members of the Coma cluster in Figure 9c (where no color constraint is used) have $B-R < 2$. Considering the sample selected where no color constraint was applied, as shown in Figure 4 and Table 2, we find that 40% of galaxies in Coma1 are confirmed cluster members, compared to only 8% in Coma3. This shows the effectiveness of $B-R$ colors in selecting potential cluster members in the cluster outskirts (ie. Coma3) where contamination by field galaxies increases. The total number of galaxies in each of these samples and the numbers of Coma cluster members are listed in Table 2. The velocity distributions for confirmed members of the Coma cluster are presented in Figure 10 for the same samples as in Figure 9. While in all three samples there is a peak at 7000 km/sec, the velocity dispersion in the Coma3 field (around the cD galaxy NGC4839) is significantly smaller than that in Coma1. This is consistent with the presence of a bound population of objects, forming the NGC 4839 group, which may be infalling towards the center of the Coma. The implications of this for the internal dynamics of the Coma cluster will be studied in a future paper in this series.

The handful of galaxies in the bright sample which have higher redshifts than that of the Coma cluster are either from the sample for which no redshifts were available (included to allocate the spare fibers), or are those with discrepant redshifts as compared to the Colless & Dunn compilation, from which the spectroscopic candidates were selected. The R-band magnitude and $B-R$ color distributions for the spectroscopically confirmed members of the cluster (both Coma1 and Coma3 fields) are presented for the bright sample (Figure 1), faint sample (Figure 3) and the sub-sample for which no color restriction was applied (Figure 4).

The photometric and spectroscopic data for galaxies in the spectroscopic survey are

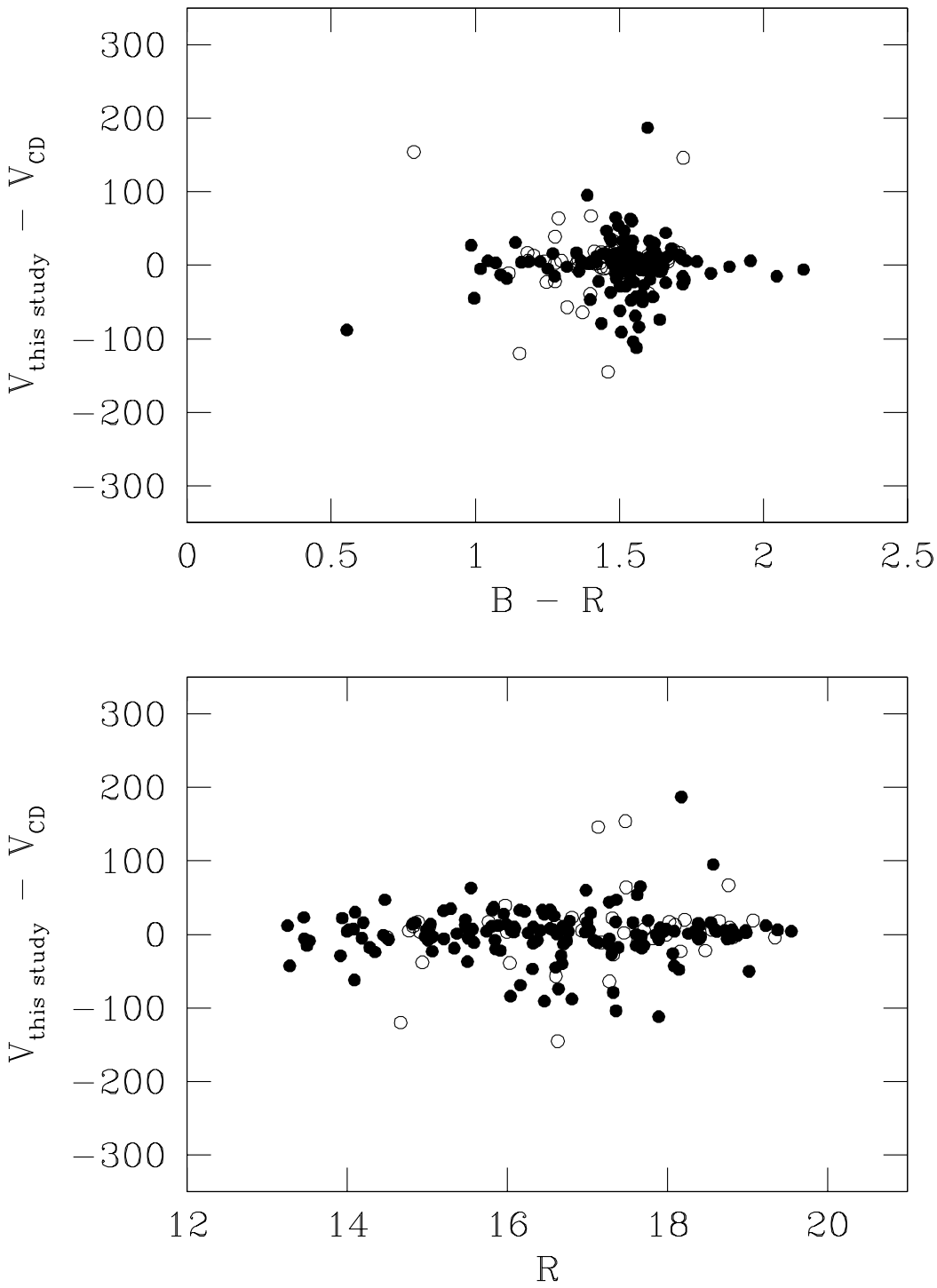

Fig. 8.— Differences between the velocities estimated in this study and those in Colless & Dunn (1996)- (V_{CD}) is presented as a function of R-band magnitude and $B - R$ color for Coma1 (solid circles) and Coma3 (open circles).

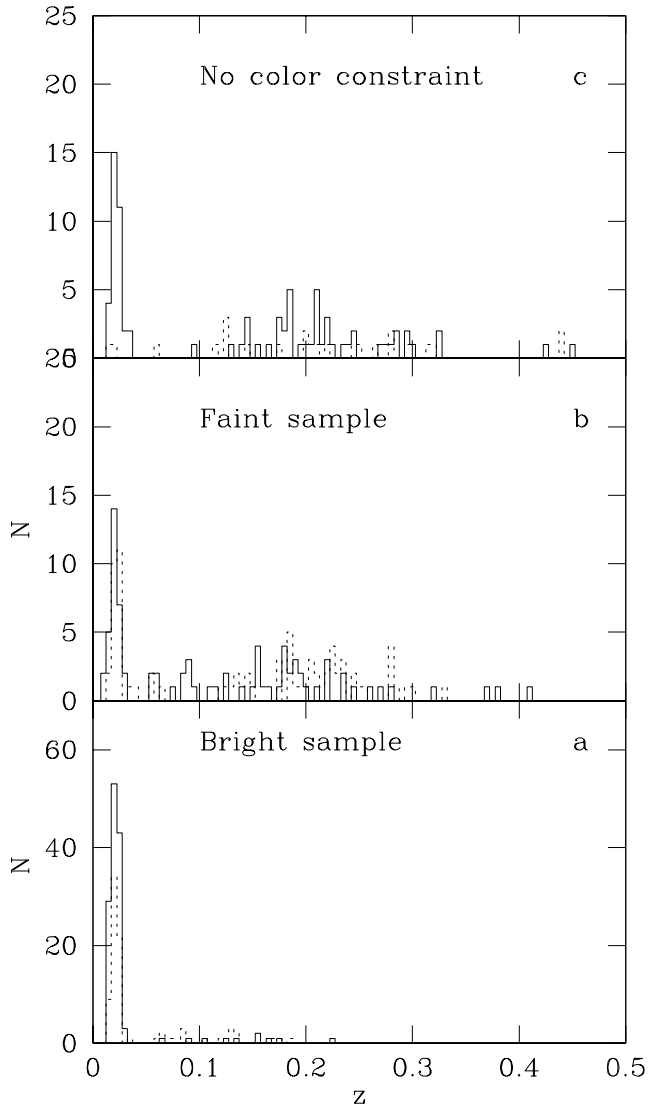

Fig. 9.— Redshift distributions for all the galaxies observed in the spectroscopic survey. The comparison is given for the three different samples with different selection criteria in this study. Objects in the Coma1 (solid line) and Coma3 (dotted line) fields are shown.

Table 2: Total number of galaxies in the spectroscopic sample and the Coma cluster members

	Coma1	Coma3
Bright Sample		
Total sample	138	85
Coma members	128	65
Faint Sample		
Total sample	83	79
Coma members	28	23
No color constraint		
Total sample	81	24
Coma members	33	2

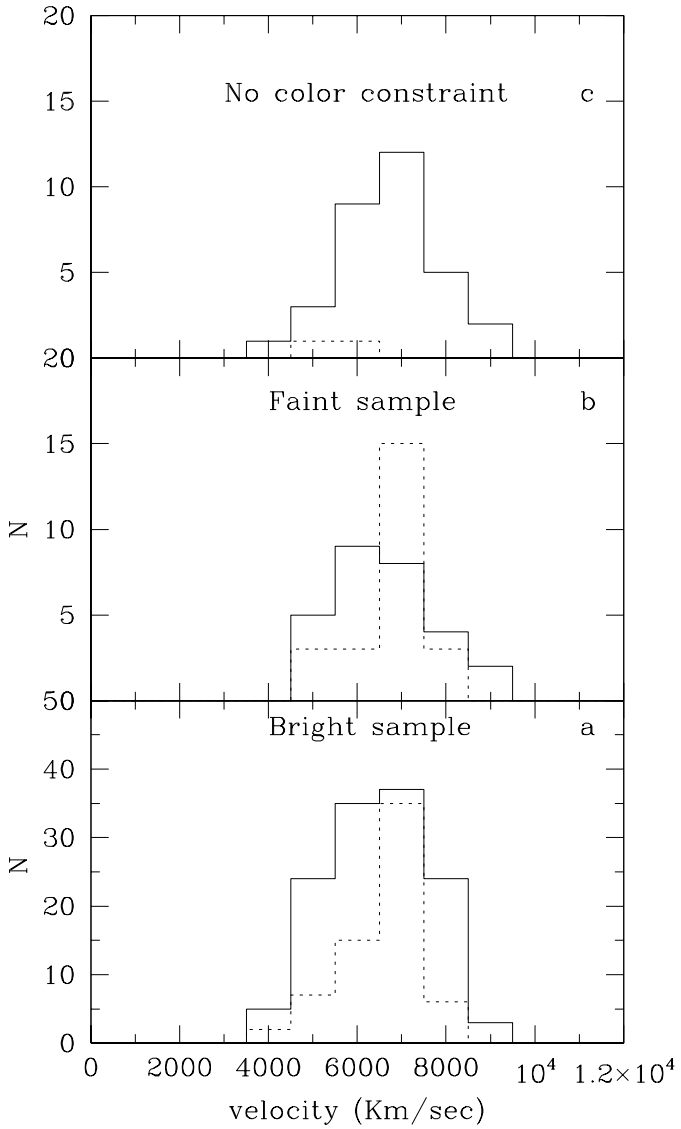

Fig. 10.— The same as Figure 9 for confirmed members of the Coma cluster. The distributions of galaxies in both the Coma1 (solid line) and Coma3 (dotted line) fields are shown.

presented in Table 3. The table includes the galaxy ID number (column 1), RA and Dec in J2000 (columns 2 and 3), distance from the cluster center [taken to be at $\alpha = 12h\ 59m\ 42.8s$ and $\delta = 27^\circ\ 58'\ 14''$ (J2000)] in degrees (column 4), R-band magnitudes and $B - R$ colors measured over a circular aperture with a diameter of 3 Kron radii (columns 5 and 6), the Kron radius in arcsec (column 7), R-band mean and effective surface brightness (columns 8 and 9), redshift (column 10), and cluster membership (column 11). Measurement of the spectral line strengths for these galaxies are discussed in paper III, with the line strengths given in a future paper in this series.

3. The completeness functions for the spectroscopic survey

Knowledge of the completeness function is needed for the future analysis of the present spectroscopic sample. Since two different selection criteria were used to conduct the spectroscopic survey, different completeness functions are needed for each of these groups.

For the bright sample, the completeness function in each luminosity interval is defined as the ratio of the number of galaxies which are *spectroscopically* confirmed members of the Coma cluster to the *expected* number of galaxies in Coma. The expected number of galaxies in the Coma cluster is estimated as the difference between the total number of galaxies in a given magnitude interval in the photometric survey and the number of galaxies in the same magnitude interval which are detected in the control field, SA57. The control field is adopted to be close to the Coma cluster and is observed in exactly the same way and to the same depth as the Coma fields. The completeness function for this sample in the combined Coma1 and Coma3 fields is presented in Figure 11.

For the faint sample, the completeness function in a given magnitude interval is defined as the ratio of the number of galaxies measured spectroscopically to the total number of galaxies in the photometric survey with $1 < \mathrm{B{-}R} < 2$. The spectroscopic completeness function for the faint sample in the combined Coma1 and Coma3 fields is also presented in Figure 11. It is clear that the bright sample is 65% complete to R=17 mag. with the completeness decreasing rapidly at fainter magnitudes, while the faint sample follows a monotonic completeness function. The faint sample is 60% complete at 18 mag, becoming increasingly incomplete towards fainter ($R \sim 19.5$) magnitudes.

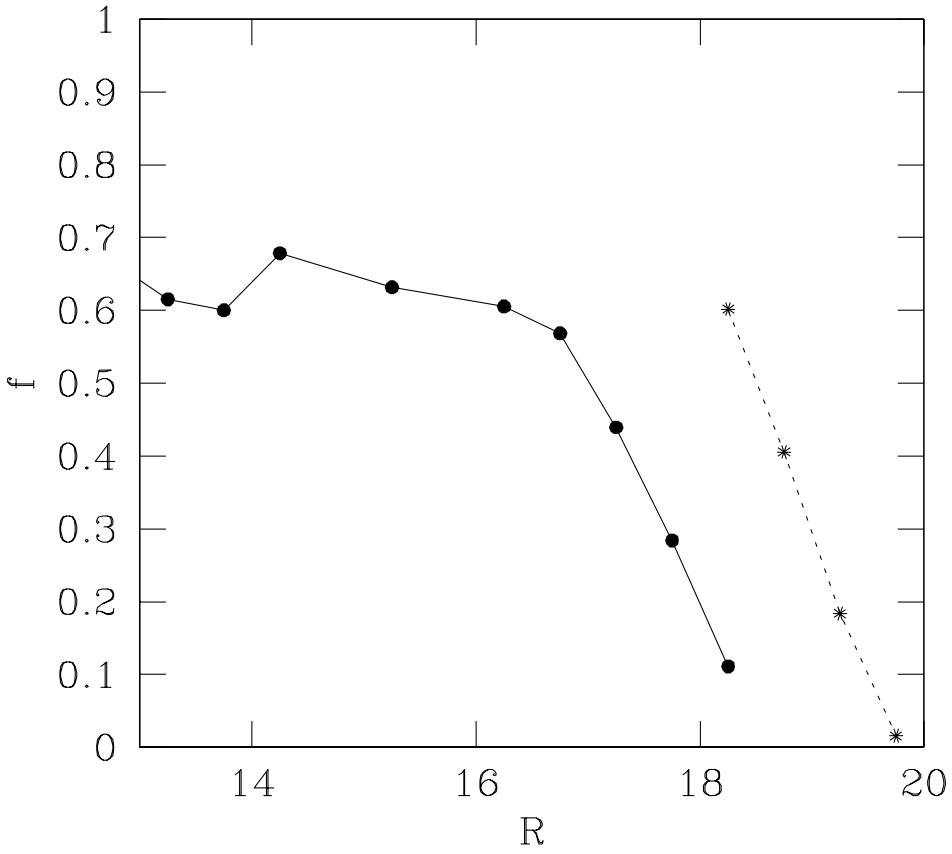

Fig. 11.— The spectroscopic completeness function for the bright (solid line) and faint (dotted line) samples.

4. Summary

Medium resolution spectroscopy (8-9 Å) was carried out for a sample of 490 galaxies of different morphological types at the core (302 galaxies) and outskirts (188 galaxies) of the Coma cluster. The galaxies cover a range in magnitude of $12 < R < 20$, corresponding to $-23 < M_R < -15$ (H_0=65 km/sec/Mpc). The candidates for spectroscopic observations were selected from our wide-angle photometric survey of the Coma cluster (paper I). Three sub-samples, with different selection criteria, were used for this purpose, consisting of; a) the 'bright sample' with $R < 18$, consisting of galaxies (drawn from a magnitude limited sample) which are spectroscopically confirmed members of the Coma cluster. For this sample, the medium resolution spectroscopy allows measurement of the spectral lines; b) the 'faint sample' satisfying the criteria $17.5 < R < 20$ and $1 < B - R < 2$. For these galaxies, we measure both the redshifts and spectral line indices; c) A random sample of galaxies with no available redshifts, where the $B - R$ color constraint is relaxed. This is to examine if the selection criteria for the 'faint sample' would exclude cluster members.

The total number of galaxies identified as spectroscopically confirmed members of the Coma cluster is 189 (at the core) and 90 (at the outskirts). Only two galaxies (in Coma1) are found with $B - R > 2$ which are members of the cluster. An analysis of the completeness function for the spectroscopic survey shows that the 'bright sample' is 65% complete at $R < 17$, becoming increasingly incomplete towards fainter magnitudes, while the 'faint sample' shows a monotonically decreasing completeness function in the range $18 < R < 20$.

Table 3. Table 3. List of the galaxies in the spectroscopic survey in Coma1(C1) and Coma3 (C3). The complete table will be presented in the ApJS paper.

ID	RA (J2000)	Dec (J2000)	r	R	B-R	r_{Kron}	μ_{mean}	μ_{eff}	z	comm
Coma1										
1144	13 0 4.95	27 33 10.48	0.426	18.152	2.503	1.496	22.72	20.53	0.3010	
1230	13 0 27.50	27 33 16.09	0.448	19.550	1.970	1.326	23.26	22.06	0.5244	
2149	13 0 25.16	27 33 7.89	0.447	16.080	1.536	3.743	22.45	20.51	0.0241	C1
2179	13 0 24.86	27 33 42.86	0.437	19.332	0.979	1.976	23.62	22.64	0.0999	
2277	12 58 41.26	27 33 34.90	0.469	18.457	1.379	2.127	23.10	21.84	0.1854	
2623	12 59 6.38	27 33 38.94	0.431	17.860	1.483	3.585	23.66	22.43	0.0265	C1
2938	12 58 39.46	27 34 0.69	0.466	19.045	2.068	1.539	23.27	22.05	0.2860	
3061	13 0 9.69	27 33 59.10	0.416	18.151	1.450	1.863	22.80	21.31	0.1653	
3368	12 59 30.74	27 34 15.93	0.402	19.920	1.165	1.282	23.49	22.42	0.1884	
.	. . .	. . .	.	.	.	.	.	.	.	
.	. . .	. . .	.	.	.	.	.	.	.	
.	. . .	. . .	.	.	.	.	.	.	.	
Coma3										
3089	12 58 24.41	26 43 46.44	1.274	20.284	2.006	1.199	23.57	22.66	0.4410	
3137	12 56 27.16	26 43 37.91	1.439	18.493	1.626	1.530	22.78	21.17	0.3015	
3160	12 58 22.57	26 43 42.06	1.277	19.375	2.845	1.369	23.37	21.61	0.3181	
3531	12 57 47.14	26 43 43.43	1.314	18.367	1.256	1.406	22.65	20.85	0.1772	
3611	12 56 19.15	26 43 32.34	1.455	16.864	1.184	3.353	22.72	21.21	0.0790	
6170	12 58 19.14	26 44 4.04	1.274	17.584	1.200	3.899	22.88	21.74	0.0708	
8304	12 56 37.00	26 44 32.90	1.407	17.999	1.577	3.096	23.59	22.67	0.0203	C3
9487	12 56 43.23	26 44 31.57	1.397	15.863	1.495	3.268	22.32	19.60	0.0233	C3
12996	12 57 50.07	26 45 50.77	1.277	18.468	1.582	1.482	22.97	20.57	0.1902	
.	. . .	. . .	.	.	.	.	.	.	.	
.	. . .	. . .	.	.	.	.	.	.	.	
.	. . .	. . .	.	.	.	.	.	.	.	

We are grateful to Matthew Colless and Richard S. Ellis for helpful discussions during the course of this work. The spectroscopic data presented in this paper are based on observations made with the William Herschel Telescope operated on the island of La Palma by the Isaac Newton Group in the Spanish Observatorio del Roque de los Muchachos of the Instituto de Astrofisica de Canarias.

REFERENCES

Barbaro, G. & Poggianti, B. M., 1997 Astron & Astrophys. 324, 490

Bridges, T. J. 1998, Fiber Optics in Astronomy III. ASP Conference Series, Vol. 152, 1998, ed. S. Arribas, E. Mediavilla, and F. Watson (1998). Proceedings of a meeting held in Puerto de la Cruz, Canary Islands, Spain, 2-4 December 1997. p.104

Caldwell, N., Rose, J. A., Sharples, R. M., Ellis, R. S., & Bower, R. 1993 AJ, 106, 473

Colless, M., Dunn, A. M. 1996 Ap. J. 458, 435

Dressler, A., Smail, I., Poggianti, B. M., Butcher, H., Couch, W. J., Ellis, R. S., Oemler, A. Jr. 1999, ApJS, 122, 51.

Godwin, J. G., Metcalfe, N., Peach, J. V., 1983, MNRAS, 202, 113

Kent, S. M. & Gunn, J. E. 1982 AJ, 87, 945

Komiyama, Y. et al. 2001, ApJ, submitted (paper I)

Poggianti, B. M., Bridges, T. J., Mobasher, B., Carter, D. et al 2001a, ApJ, in press (paper III)

Poggianti, B. M., Bridges, T. J., Carter, D., Mobasher, B. et al 2001b, ApJ., submitted

Secker, J. 1996 ApJ 469, L81

Tonry, J. Davis, M. 1979, Astron. J. 84, 1511

van Dokkum, P., Franx, M. 1998, ApJ 541, 95

van Haarlem, M. P., Cayon, L., de la Cruz, C. G., Martinez-Gonzalez, E., & Rebolo, R. 1993, MNRAS, 264, 71